Fish and Shellfish Immunology 93 (2019) 153–160

Contents lists available at ScienceDirect

Fish and Shellfish Immunology

journal homepage: www.elsevier.com/locate/fsi

Full length article

Characterization and initial functional analysis of cathepsin K in turbot (*Scophthalmus maximus* L.)

Mengyu Tian[a,1], Min Cao[a,1], Lu Zhang[a], Qiang Fu[a], Ning Yang[a], Fenghua Tan[a], Lin Song[b], Baofeng Su[c,**], Chao Li[a,*]

[a] School of Marine Science and Engineering, Qingdao Agricultural University, Qingdao, 266109, China
[b] College of Marine Science and Biological Engineering, Qingdao University of Science & Technology, Qingdao, 266011, China
[c] School of Fisheries, Aquaculture and Aquatic Sciences, Auburn University, Auburn, AL, 36849, USA

ARTICLE INFO

Keywords:
Turbot
Cathepsin K
Vibrio anguillarum
Streptococcus iniae
Microbial ligand binding ability

ABSTRACT

Cathepsins are the best-known group of proteases in lysosomes, playing a significant role in immune responses. Cathepsin K (*CTSK*) is abundantly and selectively expressed in osteoclasts, dendritic cells and monocyte-derived macrophages, where it is involved in ECM degradation and bone remodeling. A growing body of evidences have indicated the vital roles of cathepsin K in innate immune responses. Here, one *CTSK* gene was captured in turbot (*SmCTSK*) with a 993 bp open reading frame (ORF). The genomic structure analysis showed that *SmCTSK* had 7 exons similar to other vertebrate species. The syntenic analysis revealed that *CTSK* had the same neighboring genes across all the selected species, which suggested the synteny encompassing *CTSK* region was conserved during vertebrate evolution. Subsequently, *SmCTSK* was widely expressed in all the examined tissues, with the highest expression level in spleen and the lowest expression level in liver. In addition, *SmCTSK* was significantly down-regulated in intestine following Gram-negative bacteria *Vibrio anguillarum* immersion challenge, but up-regulated in three tissues (gill, skin and intestine) following Gram-positive bacteria *Streptococcus iniae* immersion challenge. Finally, the *rSmCTSK* showed strong binding ability to all the examined microbial ligands. Taken together, our results suggested *SmCTSK* played vital roles in fish innate immune responses against infection. However, the knowledge of *SmCTSK* is still limited in teleost species, further studies should be carried out to better characterize its comprehensive roles in teleost mucosal immunity.

1. Introduction

Cathepsins are one of the best known groups of proteases in lysosomes [1]. The cathepsin family mainly contains cysteine (Cys) proteases as well as serine proteases (cathepsins A and G), and aspartic proteases (cathepsins D and E). Eleven cysteine cathepsins belonging to the papain family are reported in humans, which include cathepsins B, C, F, H, K, L, O, S, V, W and X [2,3]. The transition of naive inactive zymogens of the cathepsin could be activated under specific conditions such as low pH or the presence of glycosaminoglycans. At the molecular level, the uniqueness of cathepsin K in pig, bovine and rat was shown in that it cleaves the triple helix of collagen molecules at multiple locations, an activity that is unparalleled among human collagenases [4,5]. Moreover, cathepsin K is thus by far the only papain like cysteine peptidase that has been shown to be regulated allosterically [6].

Cathepsins play significant roles in immune responses [1]. Among them, cathepsin K was originally identified as an osteoclast-specific lysosomal protease, capable of lessening the inflammatory autoimmune diseases [7]. Cathepsin K (*CTSK*) is abundantly and selectively expressed in dendritic cells and osteoclasts, where it is involved in ECM degradation and bone remodeling [8–10]. Pleiotropic roles of cathepsin K has been reported in pycnodysostosis [11], osteoporosis [12–14], cardiovascular diseases [15], adipogenesis and obesity [16], cancer [17] and embryonic development [6]. In addition, *CTSK* was also known to be involved in several important immune functions such as a direct cathepsin K-mediated bactericidal activity against intestinal bacteria in mice [18]. But only few studies have characterized its detailed immune roles against pathogen infection in teleost, piscine cathepsin K has not been completely characterized in fish immune responses against pathogen infection.

* Corresponding author.
** Corresponding author.
E-mail addresses: subfeng@auburn.edu (B. Su), leoochao@163.com (C. Li).
[1] All these authors contributed equally to this work.

https://doi.org/10.1016/j.fsi.2019.07.038
Received 7 April 2019; Received in revised form 9 July 2019; Accepted 13 July 2019
Available online 15 July 2019

Turbot (*Scophthalmus maximus* L.), one of the representative species of flatfish, is mainly distributed in the northeast of Atlantic, and was introduced into China in 1992. Following rapid development of aquaculture, it has become one of the most extensively maricultured species in China. However, bacterial diseases such as *Vibrio anguillarum*, *Streptococcus iniae*, *V. vulnificus*, *Edwardsiella tarda* and others, have resulted in high cumulative mortality and dramatic economic losses to turbot farming industry. In order to develop diseases control and prevention strategies, many efforts have been made to identify the immune-related genes in turbot, as well as their activities during bacterial infections to expand the understanding of immune mechanisms of host defense. Moreover, fish species depend more heavily on mucosal barriers than their terrestrial counterparts, as living in the pathogen-rich aquatic environment, their mucosal surfaces are continuously interacting with a broad range of commensals and primary pathogens [19]. The mucosal surfaces constitute the first immune barrier of fish host defense, thus, a better understanding of mucosal barriers is vital for aquaculture research to improve vaccine delivery via immersion or feeding [20]. Therefore, we sought here to identify and characterize the expression profiles of *CTSK* in turbot following *V. anguillarum* and *S. iniae* infection, and the binding ability to several microbial ligands. The results could expand our knowledge of the interactions between turbot and two causative bacteria, and provide new insights for molecular assistant selection for disease resistant breeding program.

2. Materials and methods

2.1. Sequence identification and analysis

The turbot *CTSK* (*SmCTSK*) transcript was captured from transcriptome and genome databases by BLAST program using *CTSK* protein sequences from other species as queries. The primers were designed based on the *CTSK* transcript sequence (Table 1). Then, the *SmCTSK* gene was translated using the online program, Open Reading Frame Finder (https://www.ncbi.nlm.nih.gov/orffinder/). The Simple Modular Architecture Research Tool (SMART) (http://smart.embl-heidelberg.de/) was used to further identified the conserved domains. The ExPASy server was used to capture the theoretical pI, molecular mass and N-glycosylation sites. MatGAT program was used to calculate the percentages of similarity and identity of turbot and other organisms' *CTSK* gene. In order to further validate the identification of *SmCTSK*, the genomic architecture of *SmCTSK* was performed using Splign (https://www.ncbi.nlm.nih.gov/sutils/splign/splign.cgi).

2.2. Phylogenetic analysis

The amino acid sequences of *CTSK* from various species including human (*Homo sapiens*), mouse (*Mus musculus*), chicken (*Gallus gallus*), Australian saltwater crocodile (*Crocodylus porosus*), frog (*Xenopus tropicalis*), fugu (*Takifugu rubripes*), half-smooth tongue sole (*Cynoglossus semilaevis*), Japanese flounder (*Paralichthys olivaceus*), medaka (*Oryzias latipes*), channel catfish (*Ictalurus punctatus*), zebrafish (*Danio rerio*) and the deduced *SmCTSK* were to construct the phylogenetic tree. ClustalW program was used to perform the multiple protein sequence alignment. Neighbor joining phylogenetic tree was constructed using the Molecular Evolutionary Genetics Analysis package (MEGA6). The tree was supported by 10,000 bootstrap repetitions using Poisson correction model and pairwise deletion of gaps.

Table 1
Primers used in this study.

Primer	Sequence (5′-3′)
qRT-PCR	
Sm-CTSK F	5′ TGTGGAGGAGGATACATGACC 3′
Sm-CTSK R	5′ GGGATTTCCTTGTAGCCTTTG 3′
18s RNA F	5′ATGGCCGTTCTTAGTTGGTG 3′
18s RNA R	5′CTCAATCTCGTGTGGCTGAA 3′
Protein expression	
Sm-CTSK-pr F	5′TGGGAACAGTGGAAGGTCGAAC 3′
Sm-CTSK-pr R	5′TCACACGACGGGGTAGCTG 3′
CDS clone	
Sm-CTSK-ORF F	5′ATGTTGCGGTTTTTGTGCG 3′
Sm-CTSK-ORF R	5′TCACACGACGGGGTAGCTG 3′

2.3. Syntenic analysis

Comparative genome syntenic analysis was conducted to further verify the identification and characterization of the genome organization of *SmCTSK*. Comparison of the neighboring genes of *SmCTSK* was performed among human, chicken, zebrafish, and turbot. The sequences of neighboring genes of *SmCTSK* were predicted from the turbot scaffold by FGENESH Program. The predicted protein sequences were annotated against NCBI non-redundant (nr) database by BLASTP program. The conserved syntenic pattern of *CTSK* gene in other species was determined in Ensemble database and Genomicus database version 95.01.

2.4. Expression of recombinant protein

To construct pEasy-*SmCTSK* plasmid, which expresses the open reading frame without signal sequence of *SmCTSK* (residues 79 to 993), the coding sequence of that region was amplified by PCR with primers (*Sm-CTSK*-pr F/R, Table 1). The target PCR product was sequenced and subcloned into the pEASY expression vector using pEASY-Blunt-E1Expression Kit (TransGen Biotech, Beijing, China). The resulting pEASY-*SmCTSK* plasmid to express histidine-tagged *SmCTSK* was subsequently transformed into *E. coli* BL21(DE3) (Novagen, USA). The *E. coli* BL21 cells were inoculated in Luria-Bertani (LB) medium at 37 °C to mid-logarithmic phase, and then induced with 0.5 mM isopropyl-β-D-thiogalactopyranoside (IPTG) at 30 °C for 6 h. Then, the His-tagged expressed recombinant *Sm*CTSK protein was purified by nickel-nitrilotriacetic acid chromatography under denaturing conditions following the manufacturer's instructions. The protein was analyzed in 12% sodium dodecyl sulfate polyacrylamide gel electrophoresis (SDS-PAGE) and stained with Coomassie Brilliant Blue R-250. The accuracy of the recombinant protein was confirmed by Western blot using standard techniques. Monoclonal mouse anti-His-tag antibody and HRP-labeled Goat Anti-Mouse IgG (GenScript, China; 1:1000 dilution) were used as primary and secondary antibodies, respectively. The specific antigen-bound antibody was visualized with DAB (Diaminobenzidine) reagent (Sigma, USA). The concentration of the purified protein was determined using Bradford's method.

2.5. Bacteria challenge and sample collection

In order to investigate the immune roles of *SmCTSK* gene in the host defense against bacterial infection, the Gram-negative bacteria *V. anguillarum* and the Gram-positive bacteria *S. iniae* were selected to conduct the bath challenge. The selected turbot fingerlings with average weight 15.6 g and length 5.5 cm were randomly divided into two groups, the challenge group that included 4 aquarium and a control group. Generally, a same procedure for the bacterial challenge followed these of our previous experiments.

For the *V. anguillarum* challenge, the fish in challenge group were immersed for 2 h at a final concentration of 5×10^7 CFU/ml and were subsequently randomly assigned to aquaria with fresh water for 2 h, 6 h, 12 h and 24 h post-challenge sample collection. For the *S. iniae* challenge, the experimental fish were challenged for 2 h by immersion at a final concentration of 5×10^6 CFU/mL and subjected to 2 h, 4 h, 8 h and 12 h post-treatment sample collection. In both challenge experiments, the control fish were immersed in sterilized media alone. At each time point, fish from the challenge and control groups were

euthanized, tissues including skin, gill and intestine from 15 fish (three replicates of 5 fish) were collected aseptically. Additionally, tissues including liver, brain, blood, head kidney and spleen from healthy turbot were also sampled. All samples were flash-frozen in liquid nitrogen and then stored in a −80 °C ultra-low freezer until preparation of RNA.

2.6. Total RNA extraction and real-time PCR analysis

Using Trizol Reagent (Invitrogen, USA), the total RNA was extracted according to the supplied instructions. The qualities of the isolated RNA were checked by electrophoresis and 1% agarose gels. The quality and quantity of RNA of each sample were also measured using Nanodrop 2000 (Thermo Electron North America LLC, FL). All extracted samples had an A260/280 ratio greater than 1.8. The total RNA was treated with RNase-free Dnase I to remove genomic DNA contamination.

In order to examine the expression patterns of *Sm*CTSK in different tissues following different bacterial challenges, the quantitative real-time PCR (qPCR) was conducted. Primer 3 online software was used to design gene specific primer (*Sm*-CTSK F/R, Table 1) based on the turbot CTSK gene sequence, and 18s gene (18 s F/R, Table 1) was used as reference gene for normalization of the expression levels. First strand cDNA was synthesized by TIANScript RT Kit (TIANGEN, China) according to the manufacturer's protocol. Quantitative real-time PCR (qPCR) was performed on a CFX96 real-time PCR detection system (Bio-Rad Laboratories, Hercules, CA) using the SYBR ExScript qRT-PCR Kit (Takara, Dalian, China) according to manufacturer's protocol. The PCR reaction mixture was performed under the following conditions: 95 °C for 30 s and followed by 40 cycles of 95 °C for 30 s, 58 °C for 30 s and followed by dissociation curve analysis, 65 °C for 5 s, then up to 95 °C at a rate of 0.1 °C/s increment, to verify the specificity of the amplicons. Triple RNA samples from healthy and infected tissues at each time point were analyzed for gene expression. Results were analyzed using Relative Expression Tool (REST®) to capture the significance at the level of $P < 0.05$. The mRNA expression levels of all samples were normalized to the level of 18s ribosomal RNA gene in the same samples.

2.7. Soild-phase enzyme-linked immunosorbent assay (ELISA)

To examine whether CSTK is a recognition receptor for microbial ligands and to evaluate the binding ability of CSTK on microbial ligands, lipopolysaccharide (LPS), lipoteichoic acid (LTA) and peptidoglycan (PGN), the enzyme-linked immunosorbent assay was performed. Each well of a 96-well microtiter plate (Corning, NY, USA) was coated with 100 μl of 5 μg/ml of LPS/LTA/PGN in coating buffer overnight at 4 °C, and then were washed with 300 μl PBST (0.05% Tween-20 in PBS) three times. Wells incubated with 100 μl of PBS were used as negative control. Each well was blocked with 100 μl of 5 mg/ml BSA at 4 °C for 1 h, and then was washed with 300 μl PBST three times. Then, the ligand-coated wells were incubated with 100 μl of a series of diluted purified recombinant *Sm*CTSK (16, 8, 4, 2, 1 and 0.5 μg/mL) at 37 °C for 1.5 h, with 4 replicates for each concentration. Subsequently, the wells were washed with 300 μl PBST three times, incubated with 100 μl mouse anti-His antibody (Solarbio, Beijing, China) (1:1000 dilution in 5 mg/ml BSA) at 37 °C for 1 h, and washed with 300 μl PBST three times. It was followed by another incubation at 37 °C for 40 min with the addition of 100 μl horseradish peroxidase-conjugated goat anti-mouse IgG (Solarbio, Beijing, China) (1:1000 dilution in 5 mg/ml BSA), then washed with PBST. The plate was visualized and measured using 0.01% of 3,3′,5,5′-Tetramethylbenzidine for 10 min. Finally, the reaction was terminated by adding 0.5 M sulfate, and the plate was then read at 450 nm wavelength with an ELISA reader. The pEASY-E1 vector protein with His-tag was used as negative control.

Table 2
Primary structural analysis. Properties of turbot CTSK determined by ProtParam.

Analysis	CTSK
No. of amino acids	330
Molecular weight (kDa)	36.4
Theoretical pI	5.18
Total number of negatively charged residues (Asp + Glu)	42
Total number of positively charged residues (Arg + Lys)	31
Formula	$C_{1596}H_{2463}N_{439}O_{494}S_{22}$
Instability index	31.87
Aliphatic index	73.91
Grand average of hydropathicity (GRAVY)	−0.363
Protein kinase C phosphorylation site	1
Casein kinase II phosphorylation site	4
N-glycosylation site	1

3. Results

3.1. Identification of turbot CTSK gene

Following molecular cloning, one *Sm*CTSK gene was captured (MK110651) with a 993 bp open reading frame (ORF) encoding 330 amino acids. The deduced *Sm*CTSK protein was predicted to have 1 protein kinase C phosphorylation site, 4 casein kinase II phosphorylation sites, and one N-glycosylation site. In addition, the deduced *Sm*CTSK protein was predicted to have a molecular mass of 36.4 kDa, a theoretical PI of 5.18 with 42 negatively charged residues (Asp + Glu), 31 positively charged residues (Arg + Lys), the instability index of 31.87 and aliphatic index of 73.91 (Table 2).

In current study, a comparison of CTSK gene structures of turbot, zebrafish, chicken and human revealed a highly conserved exon size (Fig. 1). Same number of exons of CTSK gene were observed in human, zebrafish and turbot (Fig. 1). The exon sizes of the selected species showed strong similarity and high conservation. Among the 7 exons, except for the first exon which had the largest difference for 9 bp, there were 6 exons having the same length between zebrafish and turbot; only 4 exons had the same length across all the selected species (Fig. 1). Similar exon/intron organization and distribution was observed among the selected species. However, wide variations of the CTSK orthologs in the sizes of intron existed among the interspecies. Chiefly, turbot CTSK gene has the typical genomic organization as other vertebrates.

3.2. Phylogenetic analysis

Comparison of the amino acid sequences of CTSK proteins of selected species, including mammals, teleosts, Aves, reptilia and amphibia revealed a higher level of homology at the carboxyl-terminus than at the amino-terminus. The *Sm*CTSK protein showed an overall identity of 61.9–84.2% with other CTSK proteins (Table S1). Following genomic architecture, the phylogenetic analysis was performed using MEGA6 with amino acid sequences. As shown in Fig. 2, the phylogenetic analysis results of *Sm*CTSK with other CTSK genes showed that CTSK can be divided into distinct two groups. The *Sm*CTSK as expected showed the closest relationship with CTSK in half-smooth tongue and Japanese flounder, and then with other teleost, such as medaka, and fugu. The other clade included representatives from 4 different classes, amphibia (*X. tropicalis*), Mammalia (*H. sapiens* and *M. musculus*), Aves (*G. gallus*), and Reptilia (*C. porosus*). All branching nodes were supported by high bootstrap values and the phylogenetic tree analysis was in agreement with their phylogenetic relationships (Fig. 2).

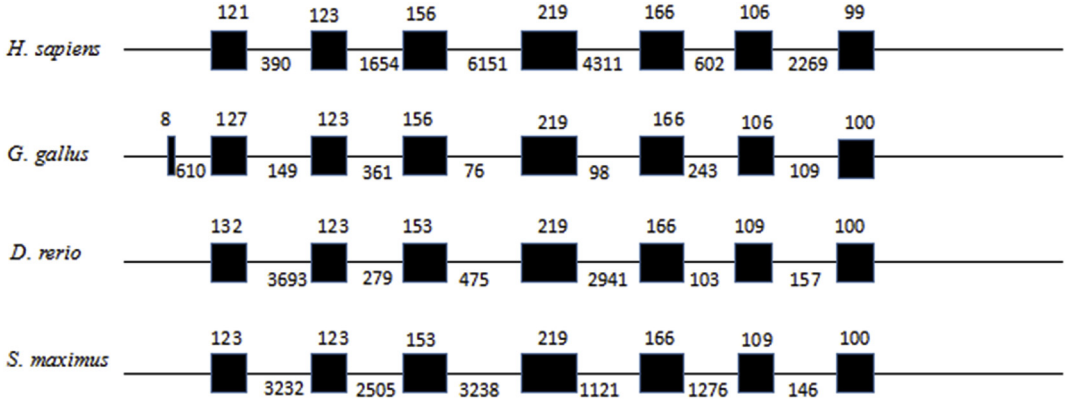

Fig. 1. Exon/intron organizations of CTSK gene were obtained by using Splign to align the cDNA sequences of human, chicken, zebrafish and turbot to their respective genomes. Boxes indicate exons and dashes indicate introns.

3.3. Syntenic analysis of SmCTSK

The syntenic analysis was performed to further validate the characterization of the *Sm*CTSK gene. As shown in Fig. 3, the same neighboring genes for *Sm*CTSK were observed in the species from mammals to reptile. In detail, the turbot CTSK gene is located on chromosome 16 and the genes adjacent to *Sm*CTSK can also be found in the homologous locus in the fugu genome (scaffold:175). A well conserved synteny was identified among all examined species under analysis, which included Induced myeloid leukemia cell differentiation protein Mcl-1 (mcl1), Alpha-endosulfine (ensa); HORMA domain-containing protein 1 (hormad1), and Cathepsin S (ctss). In addition, LysM and putative peptidoglycan-binding domain-containing protein 1 (lysmd1) and Sodium channel modifier 1 (scnm1) were also observed in the genomic neighborhood of all the mammalian species human, mouse and pig. Three genes in the analyzed genome segments, Autophagy protein 5 (atg5), Dynactin subunit 3 (dctn3) and Cytosolic 5′-nucleotidase 3A(nt5c3a), were only presented in turbot and fugu while Tumor necrosis factor alpha-induced protein 8-like protein 2 (tnfaip8l2) was only presented in fugu, human, mouse and pig (Fig. 3). In general, the turbot genome segment containing CTSK exhibits more conserved synteny to the corresponding genome segments from fugu than the mammalian segments.

3.4. The tissue distribution of SmCTSK

The tissue distribution of *Sm*CTSK was explored in 8 healthy turbot tissues including blood, liver, spleen, gill, shin, intestine, head kidney and brain by real-time PCR method. In our results, *Sm*CTSK was ubiquitously expressed in all the examined tissues. Because *Sm*CTSK was expressed at the lowest level in the liver among all tested tissues, we used expression level of liver as the baseline for comparisons. In this study, the highest expression level of *Sm*CTSK was detected in spleen with 17.83-fold, followed by head kidney (12.94-fold), skin (11.21-fold) and gill (10.35-fold), moderate expression was found in gill and blood, while the lowest expression level was detected in liver (Fig. 4).

3.5. Time-course analysis of SmCTSK expression following bacterial challenge

To further understand the immunological roles of *Sm*CTSK in turbot mucosal immunity, the expression profiles of *Sm*CTSK were examined in mucosal tissues (gill, skin and intestine) at early time points following immersion challenge with Gram-negative bacteria *V. anguillarum*, and Gram-positive bacteria *S. iniae*, respectively.

Following *V. anguillarum* challenge, *Sm*CTSK showed different expression patterns in different tissues (Fig. 5). No significant changes of the expression of *Sm*CTSK was observed in gill and skin except that the expression was repressed in gill for −2.74 fold at 12 h. In contrast, *Sm*CTSK was down-regulated in intestine, the comparatively strongest down-regulation was found at 2 h with −6.96 fold, followed by −4.19 fold at 6 h, and returned to basal level at 12 h and 24 h (Fig. 5).

In case of *S. iniae* infection, different expression pattern was observed among those three mucosal tissues. In general, the *Sm*CTSK expression levels were induced in the mucosal tissues at 4 h, 8 h and 12 h post-challenge. In detail, the up-regulated expression in gill was observed with 5.73 fold at 4 h, 5.65 fold at 8 h, and a slightly increase for 6.4 fold at 12 h. In addition, it was significantly up-regulated in skin with 4.40 fold at 4 h, and 5.00 fold at 12 h (Fig. 6). Similarly, the *Sm*CTSK showed significant up-regulation in intestine with 3.59 fold at

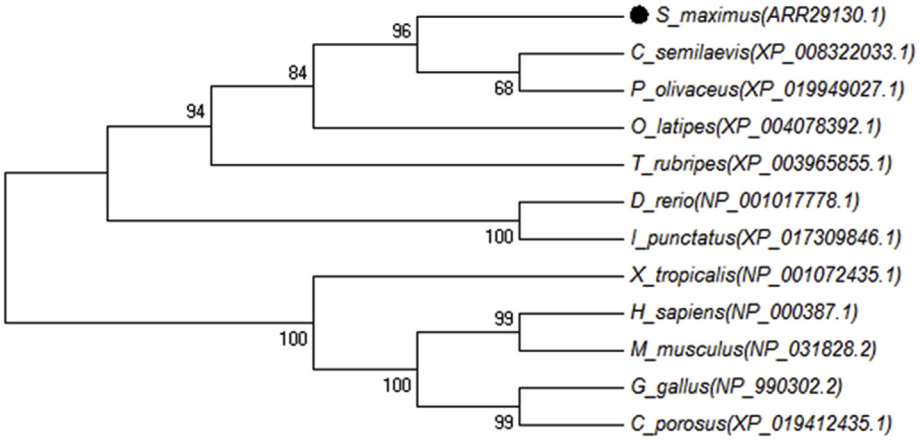

Fig. 2. Phylogenetic analysis of the turbot *CTSK* gene. The unrooted phylogenetic tree was constructed based on the amino acid sequences of cathepsin K from species of fish and other vertebrates, using the neighbor-joining method in MEGA 6. Gaps were removed by complete deletion and the phylogenetic tree was evaluated with bootstrap replications. The bootstrapping values were indicated by numbers at the nodes. Dark solid circles indicated the newly characterized turbot *CTSK* gene.

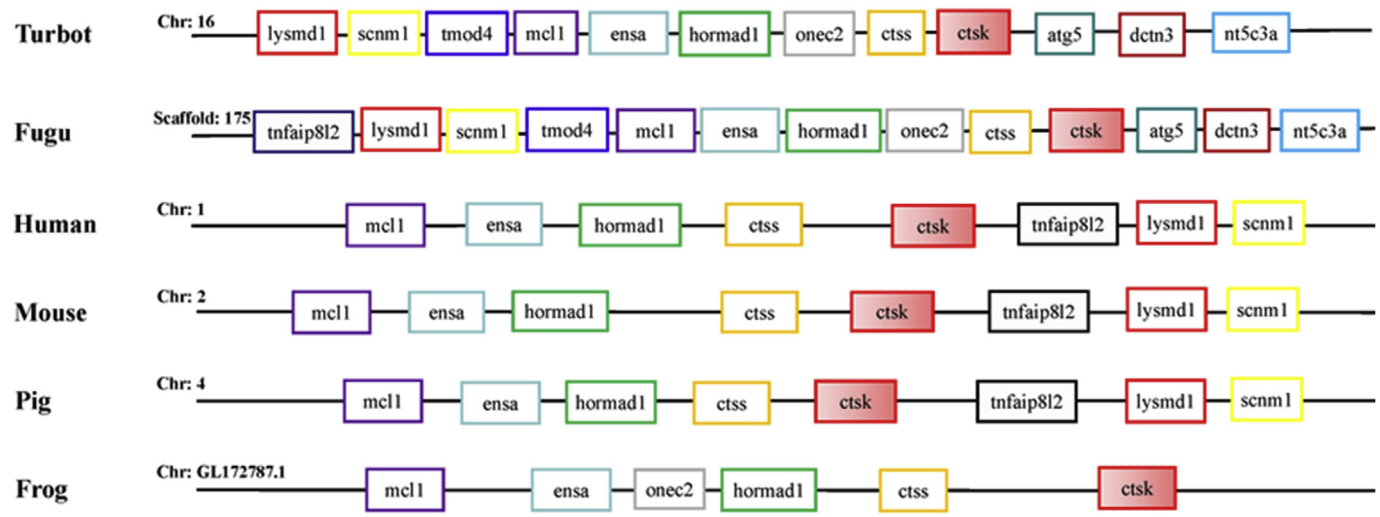

Fig. 3. Syntenic analysis of CTSK gene from turbot, fugu, human, mouse, pig and frog. The CTSK gene is highlighted by red color filled boxes. LysMd1: LysM and putative peptidoglycan-binding domain-containing protein 1; scnm1: Sodium channel modifier 1; tmod4: Tropomodulin-4; mcl1: Induced myeloid leukemia cell differentiation protein Mcl-1; ensa: Alpha-endosulfine; hormad1: HORMA domain-containing protein 1; onec2: One cut domain family member 2; ctss: Cathepsin S; ctsk: Cathepsin K; atg5: Autophagy protein 5; dctn3: Dynactin subunit 3; nt5c3a: Cytosolic 5′-nucleotidase 3A; tnfaip8l2: Tumor necrosis factor alpha-induced protein 8-like protein 2. (For interpretation of the references to color in this figure legend, the reader is referred to the Web version of this article.)

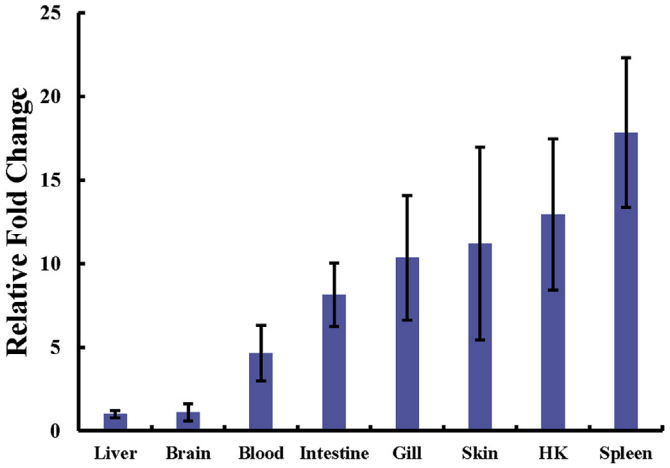

Fig. 4. Gene expression analysis of the CTSK in different healthy turbot tissues. Expression levels were calibrated against liver tissue which had the lowest expression level, and 18S rRNA was used as a reference gene. HK was the abbreviation for head kidney.

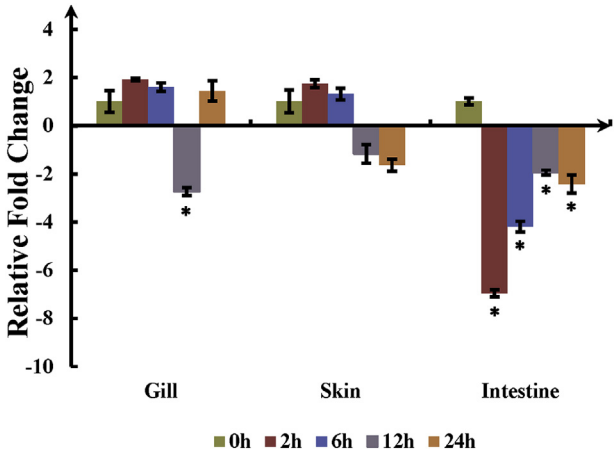

Fig. 5. Real-time qPCR analysis for CTSK expression levels following *Vibrio anguillarum* infection. The CTSK expression was measured in the mucosal tissues including skin, gill, and intestine at the time points of 2 h, 6 h, 12 h, and 24 h post-infection. Fold change was calculated by the change in expression at a given time point relative to the untreated control and normalized by change in the 18S housekeeping gene. The results were presented as mean ± SE of fold changes and * indicated statistical significance at $P < 0.05$.

4 h, and 3.6 fold at 12 h, respectively (Fig. 6).

3.6. *In vitro* microbial ligand-binding effect of recombinant SmCTSK

The *rSm*CTSK was successfully expressed and purified from *E. coli* as a native His-tagged protein. Only a single band which showed clear reaction for antisera with a molecular mass of 36.4 kDa was resolved in Western Blot analysis (Fig. 7). Then, to further validate the binding effect between *rSm*CTSK and LPS, *rSm*CTSK and PNG as well as *rSm*CTSK and LTA, ELISA was conducted. The *in vitro* binding assay demonstrated that *rSm*CTSK had strong binding ability to all the examined microbial ligands. Higher optical density values for the *rSm*CTSK binding to the microbial ligands suggested a dose-dependent response as a continuous increased absorbance with the increased concentration of *rSm*CTSK in solid-phase ELISA. The highest absorbance was found at 4.0 μg and the lowest value was found at 0.5 μg tested. The highest peak value for the binding ability of three microbial ligands was LPS, followed by PGN and LTA (Fig. 8), suggesting slightly more potent binding ability with LPS, PGN and then LTA.

4. Discussion

Cathepsins represent a very important part of the immune system. In addition to its wound healing, bone remodeling, prohormone and proenzyme activation [2,9], cathepsin K may perform more specific function in inflammatory processes and innate host defense of fish skin and muscle [21]. However, piscine cathepsin K has not been completely characterized with regard to its enzyme properties and physiological functions. Here, we describe the sequence identification and analysis, phylogenetic analysis, syntenic analysis, tissue distribution, expression profiles of *Sm*CTSK following bacterial challenge and microbial ligand-binging *in vitro* of the gene encoding for cathepsin K in the turbot.

In this study, one CTSK gene was captured in turbot (*Sm*CTSK) with similar molecular properties to other fish species. Phylogenetic analysis is known to be important aspect for gene characterization analysis, the clustered branch of turbot *Sm*CTSK with half-smooth tongue and

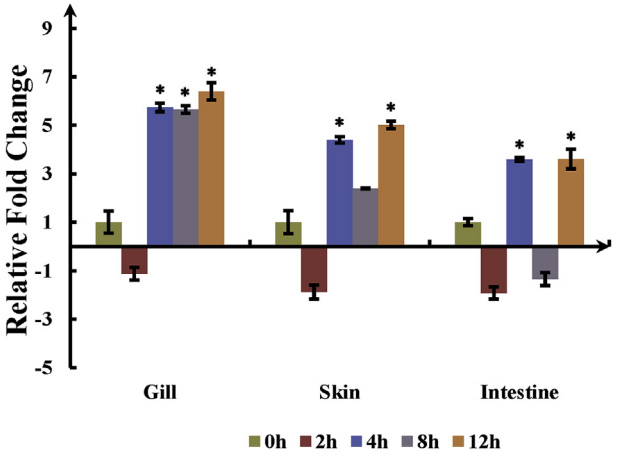

Fig. 6. Real-time qPCR analysis for CTSK expression following *Streptococcus iniae* infection. The CTSK expression levels were measured in the mucosal tissues including skin, gill, and intestine, at the time points of 2 h, 4 h, 8 h and 12 h post infection. Fold change was calculated by the change in expression at a given time point relative to the untreated control and normalized by changes in the 18S housekeeping gene. The results were presented as mean ± SE of fold changes and the * indicated statistical significance at $P < 0.05$.

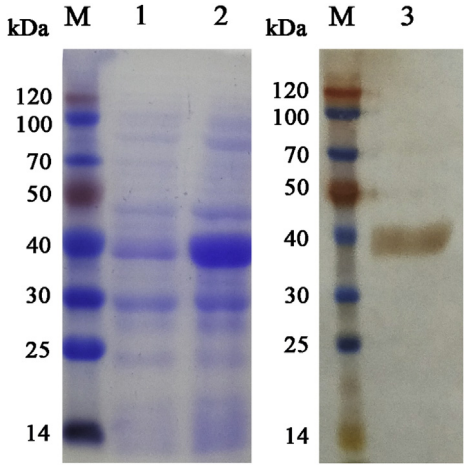

Fig. 7. SDS-PAGE analysis of the expression of the recombinant *rSm*CTSK protein. M: protein marker. Lane 1:control, SDS-PAGE analysis of the expression of *rSm*CTSK protein before induction by IPTG; lane 2: the total protein of IPTG-induced recombinant *rSm*CTSK protein; lane 3: Purified *rSm*CTSK using Western blotting analysis.

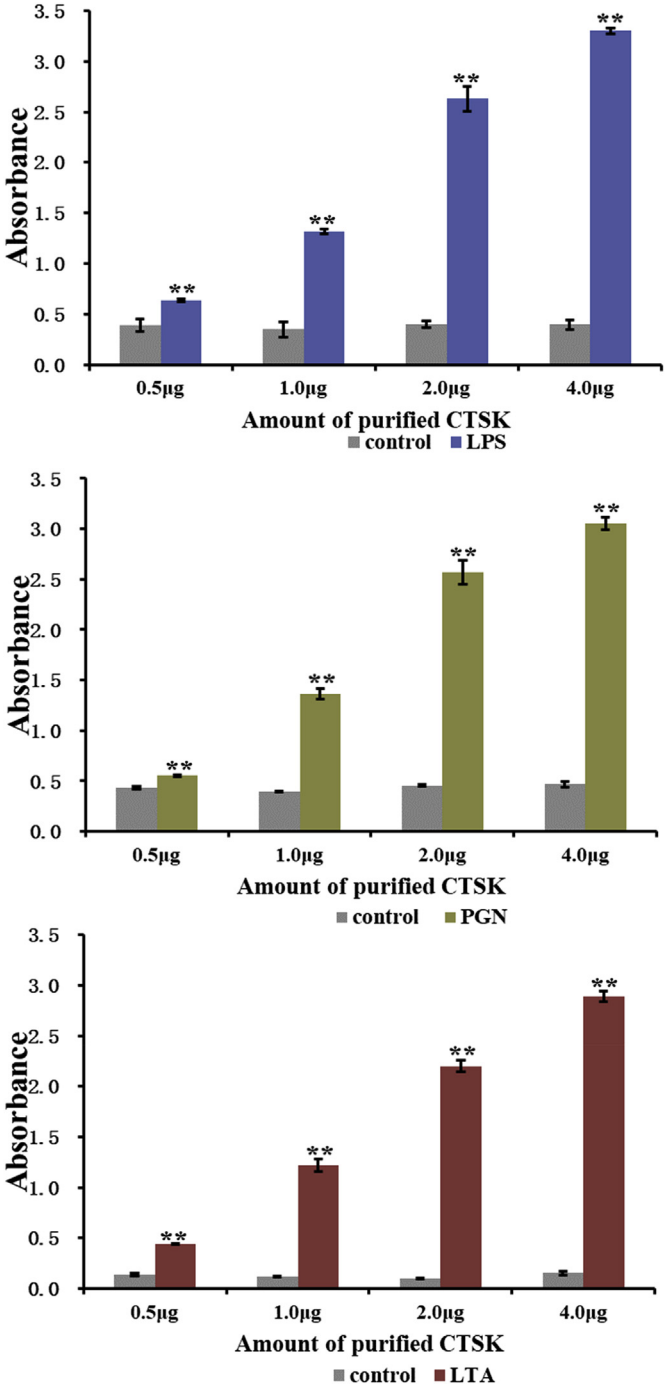

Fig. 8. Results of the *in vitro* binding assay of *Sm*CTSK to microbial ligands, including lipopolysaccharide (LPS), peptidoglycan (PGN), and lipoteichoic acid (LTA). * indicate a significant difference in the absorbance between different microbial ligands that exposed to *rSm*CTSK and the control group: $*p < 0.05$; $**p < 0.01$.

flounder and other species consolidated the identification of *Sm*CTSK. Because genomic structures changed more slowly than the sequence of proteins and other genetic characters, a deep understanding of genome structure in context of exon/intron organization of the gene and genome organization may offer more reliable inference about the gene. *Sm*CTSK possess a highly conserved exon/intron structure and has almost equivalent length of each exon to other species. In addition, high similarity of synteny genes in adjacent *Sm*CTSK on the turbot genome fragment to fugu confirmed the identification of the gene in one hand, but in another hand, dissimilarity in the synteny blocks existed among fish, mammalian species and reptiles, indication of different evolution history and event.

In human, cathepsin K expression was shown to be expressed abundantly in osteoclasts [22], lung tissues [23] and monocyte-derived macrophages [24]. In fish species, however, the tissue distribution of CTSK was rarely studied, and just in two species, i.e., goldfish [25] and olive flounder [21]. In tissue distribution analysis, *Sm*CTSK was widely expressed in all the examined tissues, with higher expression levels in spleen, head kidney and skin. In our study, the expression level of CTSK in head kidney was similarly highly as goldfish and olive flounder. Interestingly, flounder had the same relatively high expression in spleen as turbot, but not in goldfish [21,25]. It has been demonstrated that the kidney and spleen are crucial lymphoid organs or are mediated closely with the innate immune response in fish and mammals [26,27]. There are data indicating that cathepsin K may play a role in the immune system of fish skin [21]. With the limited information about relative expression profiling of CTSK in teleost, the putative roles of CTSK in other different tissues of teleost need to be further characterized and

investigated.

In order to elucidate the immune roles of *Sm*CTSK in mucosal barriers, the expression profiles of CTSK was characterized in turbot mucosal tissues (gill, skin and intestine) following bacterial infections. In case of *V. anguillarum* infection, the *Sm*CTSK showed general dramatic down-regulation in intestine. The previous studies have suggested that intestine might serve as the primary portal of entry for *V. anguillarum* [28–30], and *V. anguillarum* bacteria could be detected in spleen in more than 50% of orally infected fish [30]. In zebrafish following immersion infection, the intestine was the first site where the pathogen was detected [31]. Moreover, following bath-vaccination of live attenuated *V. anguillarum* vaccine, bacterial cells proliferated rapidly in 3 h after vaccination and maintained at a high level until 6 h in the intestine, with a significant up-regulation of TLR5 triggering MyD88-dependent signaling pathway in the intestine [32]. In turbot, an oral administration of *V. anguillarum* for turbot larvae could lead to significant mortality [33]. Following administration of *V. anguillarum* by anal or intragastric intubation, the bacteria could be detected in turbot spleen as early as 2 h, suggesting the quick pass ability of such bacteria through the intestine mucosal barriers [34]. Here, the significant down-regulation of CTSK in turbot intestine following *V. anguillarum* challenge suggested its vital roles in intestinal immune responses. Further effort is in need to examine whether turbot CTSK may play similar roles in intestine as mammals and other fishes.

After *S. iniae* infection, significant up-regulation, instead of repression post *V. anguillarum* challenge, was observed in mucosal tissues at all examined time points except 2 h for *Sm*CTSK, revealing the different strategies *Sm*CTSK might utilize against two bacterial infections. In tilapia, relative expression level of Cathepsin K was up-regulated in spleen at 5 h following *S. agalactiae* challenge (anther streptococci strain) [35], suggesting different virulent mechanisms of streptococci species and specific stimulated immune response between host and pathogen. Although our understanding of the molecular interactions between *S. iniae* and turbot is still limited, our data indicated that cathepsin K may be related to immune system and confer a more specific function in innate host defense.

In order to better understand the role of *rSm*CTSK in host defense against various pathogens, microbial binding effects of three representative microbial ligands (LPS, LTA and PGN) were evaluated *in vitro*. The recombinant protein *rSm*CTSK was successfully expressed, its molecular mass was in agreement with that predicted using the bioinformatic tools. *rSm*CTSK bound to three microbial ligands with comparatively high affinity, suggesting a vital important role that *Sm*CTSK might be involved in the sensing and phagocytosis of bacterial pathogens. Interestingly, CTSA and CTSZ in turbot also have strong binding to microbial ligands [36,37]. To our best knowledge the binding of CTSK to microbial ligands was investigated for the first time in teleost.

Cathepsin L family, including cathepsins L, S, and K evolved from a common ancestral gene before mammalian divergence because the much higher conserved mammals orthologs than those among paralogs were found in the phylogenetic analysis [38]. Cathepsin S and L are both implicating the functional specificity of antigen processing in immune system. Function of cathepsin S has been associated with muscle protein degradation [39], antigen processing [40], and pathogen defense [41]. Cathepsin K was found in the intestinal goblet cells and mucin layer, and thus confers an intestinal antibacterial property in mice [18]. Such direct cathepsin K-mediated bactericidal activity against intestinal bacteria ameliorates the severity of the intestinal inflammation. In fish, cathepsin K has also been shown to be involved in several important functions, including the osteoclastic marker expressed in multinucleate osteoclasts of goldfish [42], zebrafish [43] and medaka [44]. However, a number of issues are awaiting to be addressed before achieving a better characterization of CTSK roles in teleost mucosal immunity.

In conclusion, the *SmCTSK* gene was examined in turbot by analyzing the genomic structure, tissue-specific expression patterns, *in vivo* gene expression after *V. anguillarum* and *S. iniae* infection, and evaluation of the binding effect to microbial ligands *in vitro*. Collectively, these results offer new insight for understanding and investigating the molecular function of turbot *CTSK*, especially in further exploring the mucosal immunity and interactions between the host and pathogen.

Acknowledgement

This study was supported by the Scientific and Technological Innovation of Blue Granary (2018YFD0900503), the National Science Foundation of China (No.:31602193), the keypoint research and invention program in Shandong Province (2017GHY215004), and it was financially supported also by “First class fishery discipline” programme in Shandong Province, China.

Appendix A. Supplementary data

Supplementary data to this article can be found online at https://doi.org/10.1016/j.fsi.2019.07.038.

References

[1] S. Conus, H.U. Simon, Cathepsins and their involvement in immune responses, Swiss Med. Wkly. 140 (2010) w13042.
[2] V. Turk, B. Turk, D. Turk, Lysosomal cysteine proteases: facts and opportunities, EMBO J. 20 (17) (2001) 4629–4633.
[3] A. Rossi, Q. Deveraux, B. Turk, A. Sali, Comprehensive search for cysteine cathepsins in the human genome, Biol. Chem. 385 (5) (2004) 363–372.
[4] W. Kafienah, D. Brömme, D.J. Buttle, L.J. Croucher, A.P. Hollander, Human cathepsin K cleaves native type I and II collagens at the N-terminal end of the triple helix, Biochem. J. 331 (Pt 3) (1998) 727–732.
[5] P. Garnero, O. Borel, I. Byrjalsen, M. Ferreras, F.H. Drake, M.S. McQueney, et al., The collagenolytic activity of cathepsin K is unique among mammalian proteinases, J. Biol. Chem. 273 (48) (1998) 32347–32352.
[6] M. Novinec, B. Lenarčič, Cathepsin K: a unique collagenolytic cysteine peptidase, Biol. Chem. 394 (9) (2013) 1163–1179.
[7] M. Asagiri, T. Hirai, T. Kunigami, S. Kamano, H.J. Gober, K. Okamoto, et al., Cathepsin K-dependent toll-like receptor 9 signaling revealed in experimental arthritis, Science 319 (5863) (2008) 624–627.
[8] Y. Yasuda, J. Kaleta, D. Brömme, The role of cathepsins in osteoporosis and arthritis: rationale for the design of new therapeutics, Adv. Drug Deliv. Rev. 57 (7) (2005) 973–993.
[9] T. Zavasnik-Bergant, B. Turk, Cysteine proteases: destruction ability versus immunomodulation capacity in immune cells, Biol. Chem. 388 (11) (2007) 1141–1149.
[10] U. Grabowskal, T.J. Chambers, M. Shiroo, Recent developments in cathepsin K inhibitor design, Curr. Opin. Drug Discov. Dev 8 (5) (2005) 619–630.
[11] P. Saftig, E. Hunziker, O. Wehmeyer, S. Jones, A. Boyde, W. Rommerskirch, et al., Impaired osteoclastic bone resorption leads to osteopetrosis in cathepsin-K-deficient mice, Proc. Natl. Acad. Sci. U. S. A. 95 (23) (1998) 13453–13458.
[12] H. Bone, Future directions in osteoporosis therapeutics, Endocrinol Metab. Clin. N. Am. 41 (3) (2012) 655–661.
[13] S. Boonen, E. Rosenberg, F. Claessens, D. Vanderschueren, S. Papapoulos, Inhibition of cathepsin K for treatment of osteoporosis, Curr. Osteoporos. Rep. 10 (1) (2012) 73–79.
[14] K. Lippuner, The future of osteoporosis treatment - a research update, Swiss Med. Wkly. 142 (2012) w13624.
[15] A.O. Samokhin, A. Wong, P. Saftig, D. Brömme, Role of cathepsin K in structural changes in brachiocephalic artery during progression of atherosclerosis in apoE-deficient mice, Atherosclerosis 200 (1) (2008) 58–68.
[16] C. Chiellini, M. Costa, S.E. Novelli, E.Z. Amri, L. Benzi, A. Bertacca, et al., Identification of cathepsin K as a novel marker of adiposity in white adipose tissue, J. Cell. Physiol. 195 (2) (2003) 309–321.
[17] K. Husmann, R. Muff, M.E. Bolander, G. Sarkar, W. Born, B. Fuchs, Cathepsins and osteosarcoma: expression analysis identifies cathepsin K as an indicator of metastasis, Mol. Carcinog. 47 (1) (2008) L66–L73.
[18] C. Sina, S. Lipinski, O. Gavrilova, K. Aden, A. Rehman, A. Till, et al., Extracellular cathepsin K exerts antimicrobial activity and is protective against chronic intestinal inflammation in mice, Gut 62 (4) (2013) 520–530.
[19] G.D. Gómez, B. Balcázar, A review on the interactions between gut microbiota and innate immunity of fish, FEMS Immunol. Med. Microbiol. 52 (2) (2010) 145–154.
[20] E. Peatman, M. Lange, H. Zhao, B.H. Beck, Physiology and immunology of mucosal barriers in catfish (Ictalurus spp.), Tissue Barriers 3 (4) (2015) e1068907.
[21] J.E. Je, S.J. Ahn, N.Y. Kim, J.S. Seo, M.S. Kim, N.G. Park, et al., Molecular cloning, expression analysis and enzymatic characterization of cathepsin K from olive flounder (*Paralichthys olivaceus*), Comp. Biochem. Physiol. Mol. Integr. Physiol. 154 (4) (2009) 474–485.
[22] A. Littlewood-Evans, T. Kokubo, O. Ishibashi, T. Inaoka, B. Wlodarski, J.A. Gallagher, et al., Localization of cathepsin K in human osteoclasts by in situ

hybridization and immunohistochemistry, Bone 20 (2) (1997) 81–86.
[23] T. Inaoka, G. Bilbe, O. Ishibashi, K. Tezuka, M. Kumegawa, T. Kokubo, Molecular cloning of human cDNA for cathepsin K: novel cysteine proteinase predominantly expressed in bone, Biochem. Biophys. Res. Commun. 206 (1) (1995) 89–96.
[24] G.P. Shi, H.A. Chapman, S.M. Bhairi, C. DeLeeuw, V.Y. Reddy, S.J. Weiss, Molecular cloning of human cathepsin O, a novel endoproteinase and homologue of rabbit OC2, FEBS Lett. 357 (2) (1995) 129–134.
[25] R. Harikrishnan, M.C. Kim, J.S. Kim, Y.J. Han, I.S. Jang, C. Balasundaram, et al., Immune response and expression analysis of cathepsin K in goldfish during *Aeromonas hydrophila* infection, Fish Shellfish Immunol. 28 (4) (2010) 511–516.
[26] G.H. Curtis, D.G. Gall, Macromolecular transport by rat gastric mucosa, Am. J. Physiol. 262 (6 Pt 1) (1992) G1033–G1040.
[27] J. Zou, M.S. Clark, C.J. Secombes, Characterisation, expression and promoter analysis of an interleukin 10 homologue in the puffer fish, *Fugu rubripes*, Immunogenetics 55 (5) (2003) 325–335.
[28] X. Cai, C. Gao, B. Su, F. Tan, N. Yang, G. Wang, Expression profiling and microbial ligand binding analysis of high-mobility group box-1 (HMGB1) in turbot (*Scophthalmus maximus* L.), Fish Shellfish Immunol. 78 (2018) 100–108.
[29] C. Li, C. Gao, Q. Fu, B. Su, J. Chen, Identification and expression analysis of fetuin B (FETUB) in turbot (*Scophthalmus maximus* L.) mucosal barriers following bacterial challenge, Fish Shellfish Immunol. 68 (2017) 386–394.
[30] C. Gao, B. Su, D. Zhang, N. Yang, L. Song, Q. Fu, et al., l-rhamnose-binding lectins (RBLs) in turbot (*Scophthalmus maximus* L.): characterization and expression profiling in mucosal tissues, Fish Shellfish Immunol. 80 (2018) 264–273.
[31] R. O'Toole, J. Von Hofsten, R. Rosqvist, P.E. Olsson, H. Wolf-Watz, Visualisation of zebrafish infection by GFP-labelled *Vibrio anguillarum*, Microb. Pathog. 37 (1) (2004) 41–46.
[32] X. Liu, H. Wu, X. Chang, Y. Tang, Q. Liu, Y. Zhang, Notable mucosal immune responses induced in the intestine of zebrafish (*Danio rerio*) bath-vaccinated with a live attenuated *Vibrio anguillarum* vaccine, Fish Shellfish Immunol. 40 (1) (2014) 99–108 2014.
[33] M. Chair, M. Dehasque, S. Van Poucke, H. Nelis, P. Sorgeloos, A.P. De Leenheer, An oral challenge for turbot larvae with *Vibrio anguillarum*, Aquacult. Int. 2 (4) (1994) 270–272.
[34] J.C. Oisson, A. Jöborn, A. Westerdahl, L. Blomberg, S. Kjelleberg, P.L. Conway, Is turbot, *Scophthalmus maximus* (L.), intestine a portal of entry for the fish pathogen *Vibrio anguillarum*? J. Fish Dis. 19 (3) (2010) 225–234.
[35] J. Zhu, Q. Fu, Q. Ao, Y. Tan, Y. Luo, H. Jiang, et al., Transcriptomic profiling analysis of tilapia (*Oreochromis niloticus*) following *Streptococcus agalactiae* challenge, Fish Shellfish Immunol. 62 (2017) 202–212.
[36] Q. Fu, N. Yang, C. Gao, M. Tian, S. Zhou, X. Mu, et al., Characterization, expression signatures and microbial binding analysis of cathepsin A in turbot, *Scophthalmus maximus* L. (SmCTSA), Fish Shellfish Immunol. 81 (2018) 21–28.
[37] X. Cai, C. Gao, H. Song, N. Yang, Q. Fu, F. Tan, et al., Characterization, expression profiling and functional characterization of cathepsin Z (CTSZ) in turbot (*Scophthalmus maximus* L.), Fish Shellfish Immunol. 84 (2019) 599–608.
[38] P.J. Berti, A.C. Storer, Alignment/phylogeny of the papain superfamily of cysteine proteases, J. Mol. Biol. 246 (2) (1995) 273–283.
[39] M. Yamashita, S. Konagaya, High activities of cathepsins B, D, H, and L in the white muscle of chum salmon in spawning migration, Comp. Biochem. Physiol. B 95 (1) (1990) 149–152.
[40] T.S. Uinuk-Ool, N. Takezaki, N. Kuroda, F. Figueroa, A. Sato, I.E. Samonte, et al., Phylogeny of antigen-processing enzymes: cathepsins of a cephalochordate, an agnathan and a bony fish, Scand. J. Immunol. 58 (4) (2003) 436–448.
[41] F. Aranishi, Lysis of pathogenic bacteria by epidermal cathepsins L and B in the Japanese eel, Fish Physiol. Biochem. 20 (1) (1999) 37–41.
[42] K. Azuma, M. Kobayashi, M. Nakamura, N. Suzuki, S. Yashima, S. Iwamuro, et al., Two osteoclastic markers expressed in multinucleate osteoclasts of goldfish scales, Biochem. Biophys. Res. Commun. 362 (3) (2007) 594–600.
[43] D.M. Parichy, D.G. Ransom, B. Paw, L.I. Zon, S.L. Johnson, An orthologue of the *kit*-related gene *fms* is required for development of neural crest-derived xanthophores and a subpopulation of adult melanocytes in the zebrafish, *Danio rerio*, Development 127 (14) (2000) 3031–3044.
[44] Y. Nemoto, K. Higuchi, O. Baba, A. Kudo, Y. Takano, Multinucleate osteoclasts in medaka as evidence of active bone remodeling, Bone 40 (2) (2007) 399–408.